Title: Muscarinic modulation of the *Xenopus laevis* tadpole spinal mechanosensory pathway

Authors: Nicola Jean Porter, Wen-Chang Li

PII: S0361-9230(18)30077-7
DOI: https://doi.org/10.1016/j.brainresbull.2018.03.015
Reference: BRB 9401

To appear in: *Brain Research Bulletin*

Received date: 1-2-2018
Revised date: 19-3-2018
Accepted date: 24-3-2018

Please cite this article as: Nicola Jean Porter, Wen-Chang Li, Muscarinic modulation of the Xenopus laevis tadpole spinal mechanosensory pathway, Brain Research Bulletin https://doi.org/10.1016/j.brainresbull.2018.03.015

Muscarinic modulation of the *Xenopus laevis* tadpole spinal mechanosensory pathway

Nicola Jean Porter, Wen-Chang Li*

* wl21@st-andrews.ac.uk, School of Psychology and Neuroscience, the University of St Andrews, St Mary's Quad, South Street, St Andrews, Fife, KY16 9JP, UK.

Highlights

- Carbachol does not affect properties of sensory Rohon-Beard neurons.
- Carbachol hyperpolarises sensory interneurons and decreases their input resistance.
- Carbachol increases thresholds for swimming initiation by skin stimulation.
- There lacks endogenous activation of muscarinic receptors in early development.

Abstract

Muscarinic acetylcholine receptors (mAChRs) mediate effects of acetylcholine (ACh) in many systems, including those involved in spinal functions like locomotion. In *Xenopus laevis* tadpoles at two days old, a model vertebrate for motor control research, we investigated the role of mAChRs in the skin mechanosensory pathway. We found that mAChR activation by carbachol did not affect the sensory Rohon-Beard neuron properties. However, carbachol could hyperpolarise sensory interneurons and decrease their voltage responses to outward currents. Carbachol could increase the threshold for the mechanosensory pathway to start swimming,

preventing the initiation of swimming at higher concentrations altogether. Recording from the sensory interneurons in carbachol showed that their spiking after skin stimulation was depressed. However, the general muscarinic antagonist atropine did not have a clear effect on the swimming threshold or the modulation of sensory interneuron membrane conductance. Our results suggest the skin mechanosensory pathway may be subject to muscarinic modulation in this simple vertebrate system.

Abbreviations

mAChR, Muscarinic acetylcholine receptors; nAChR, nicotinic acetylcholine receptor; dli, dorsolateral interneuron; dlc, dorsolateral commissural interneuron; dla, dorsolateral ascending interneuron; EPSP, Excitatory postsynaptic potential; IPSP, inhibitory postsynaptic potential; R_{inp-}, cellular input resistance tested using negative step currents; R_{inp+}, cellular input resistance tested using positive step currents; RB, Rohon-Beard neuron; I-V, current-voltage; v.r., ventral root; PBS, phosphate buffer saline; AHP, afterhyperpolarisation; K_{or}, outward-rectifying potassium currents; DAB, 3,3'-diaminobenzidine; MN, motoneuron; aIN, ascending interneuron; TTX, tetrodotoxin

Keywords*: Xenopus laevis*; swimming; muscarinic receptor; rectification; carbachol; mechanosensory

Introduction

The vertebrate spinal cord contains a variety of neurons with many different transmitter phenotypes. The main excitatory neurotransmitter is glutamate but there have been studies of excitatory cholinergic transmission in several vertebrate species.

Cholinergic transmission within the mammalian spinal cord can originate from the motoneuron (MN) central axon branches and some cholinergic interneurons in the dorsal horn and surrounding the central canal (Sherriff & Henderson, 1994; Arvidsson *et al.*, 1997; Huang *et al.*, 2000; Zagoraiou *et al.*, 2009). In contrast, cholinergic inputs to the spinal cord are less clear in non-mammalian vertebrates.

Although it has been shown that spinal cholinergic transmission can be mediated by nicotinic cholinergic receptors (nAChR) (Li *et al.*, 2004b; Mentis *et al.*, 2005; Nishimaru *et al.*, 2005), many cholinergic effects in the spinal cord are mediated by muscarinic receptors (mAChR). mAChRs have been shown to be expressed in the ventral horn of the mammalian spinal cord (Yung & Lo, 1997; Wilson *et al.*, 2004). In the neonatal rat spinal circuit, muscarinic cholinergic transmission from commissural neurons could increase MN output during fictive locomotion by activating M_2, M_3, and M_4 receptors (Bertrand & Cazalets, 2011). The activation of M_2 receptors located at mouse C-bouton synapses (Zagoraiou *et al.*, 2009) reduces the size of the MN spike afterhyperpolarisation (AHP) and increases MN excitability (Miles *et al.*, 2007). Similar modulation of AHP amplitude has been reported in cats and rats (Brownstone *et al.*, 1992; Schmidt, 1994). With regards to non-mammalian species, in turtle lumbar MNs, rhythmic activity could be produced by application of both muscarinic and nicotinic agents and cholinergic activation has been found to increase neuron excitability by modulating K^+ and Ca^{2+} currents (Guertin & Hounsgaard, 1999; Alaburda *et al.*, 2002). In the isolated mudpuppy spinal cord, application of the muscarinic agonist carbachol had no effect on the resting preparation but carbachol disrupted rhythmic activity induced by NMDA application, which could be blocked by atropine (Fok & Stein, 2002). In the isolated lamprey spinal cord, ACh has been

shown to modulate swimming rhythms by altering burst intensity and cycle period (Quinlan *et al.*, 2004), which were mediated predominantly by nAChRs but had a mAChR-mediated component. Further study found that this modulation resulted from pre- and postsynaptic nAChR and mAChR activation, arising from ACh release by MNs and spinal interneurons (Quinlan & Buchanan, 2008). Some brainstem level of muscarinic control of lamprey swimming has also been identified (Smetana *et al.*, 2007; Smetana *et al.*, 2010).

Cholinergic transmission has previously been studied in the *Xenopus laevis* tadpole swimming circuit. In isolated spinal cord preparations, ACh could increase spontaneous swimming incidence, which could be reversed by atropine (Panchin Yu *et al.*, 1991). Later it was shown in MNs that activating nAChRs caused depolarisation while muscarinic agonist application led to slight hyperpolarisation in the presence of tetrodotoxin (TTX), suggesting MNs possess both nAChRs and mAChRs (Perrins & Roberts, 1994). In this study, we found carbachol could increase tadpole swimming threshold and investigated the underlying cellular mechanisms in the mechanosensory pathway.

Materials and methods

Xenopus laevis tadpoles were obtained by inducing mating in pairs of adult frogs using human chorionic gonadotropin (Sigma-Aldrich, UK). All experimental procedures were approved by a local Animal Welfare Ethics committee and comply with UK Home Office regulations. Embryos were stored at low density in trays of dechlorinated tap water. To stagger development and allow different stages of tadpole

to be used in experiments the eggs were kept at a range of temperatures (typically 16-23°C). Tadpoles were selected when they had developed to stage 37/38 (Nieuwkoop & Faber, 1956). Animals were first anaesthetised in a 0.1% ethyl 3-aminobenzoate methanesulfonate (Sigma-Aldrich, UK) before being pinned onto a rotatable silicon elastomer stage (Sylgard; Dow Corning, USA) in a saline bath (saline composition in mM: NaCl, 115; KCl, 3; Hepes, 10; $CaCl_2$, 2; $MgCl_2$, 1; $NaHCO_3$, 2.4 at pH 7.4). The dorsal fin was slit using a sharp tungsten dissection needle to facilitate action of the neuromuscular blocker α-bungarotoxin at 10μM (Tocris Bioscience, UK). Once immobilised, tadpoles were re-pinned to the Sylgard stage for dissection. Pins were typically placed in the eye, through the notochord just caudal to the otic capsule and in the caudal trunk region. Dissections for both extracellular and intracellular recordings were carried out using custom-etched tungsten needles.

The majority of the yolk belly was removed along with the skin covering the myotomes of both sides in the trunk region (Fig.1A). Skin covering the head and tail of the animal was not removed to provide sites for electrical stimulation. Muscle myotomes on both sides of the trunk were removed to expose the spinal cord. A few myotomes were retained caudally to allow recording of ventral root (v.r.) activity. Melanophores covering the spinal cord were removed for greater visibility of spinal neurons. The spinal cord was opened dorso-ventrally by placing a sharp tungsten needle between the two halves of the cord and following the path of the neurocoel. Once the cord was opened a finer dissection needle was used to remove ependymal cells that line the neurocoel, thus allowing patch electrode access to the exposed somata of spinal neurons (Fig.1A). Once dissections were complete the animals were moved to a smaller rotatable Sylgard stage in a recording bath (2ml) perfused with

saline. Circulation was maintained using a Masterflex C/L pump (Cole Parmer, UK) at a rate of about 2ml per minute.

All recordings were carried out under an Olympus BX51W1 upright microscope (Olympus Microscopy, UK). The preparation was visualised using x4 (v.r. recordings) and x40 water immersion (whole-cell recordings) lenses. v.r. activity was recorded using glass suction electrodes placed on the intermyotomal clefts, wherein lie the motor neuron axons. Electrical stimulation to evoke fictive swimming was delivered through a Digitimer DS3 isolated stimulator (Digitimer Ltd, UK). Fictive swimming could also be induced via the pineal eye pathway by light dimming (Roberts, 1978). Control, drug circulation and wash conditions were each maintained for 20 minutes in extracellular recordings unless stated, with the exception of antagonist experiments in which the wash period was extended to 40 minutes. Following an episode of swimming the animal was allowed to rest for 2 minutes before another stimulus was applied. When the swimming initiation threshold was increased by carbachol, the stimulating current was manually increased incrementally in amplitude and delivered within seconds until swimming was initiated or the current limit of 32 mA was reached. RB neuron synapses show clear short-term depression when RB neurons fire at 10-40 Hz. At < 3 Hz, however, there is little short-term plasticity in RB EPSPs (Li, unpublished observations). Therefore, these consecutive stimuli should not significantly alter swimming initiation threshold by affecting sensory information processing in the sensory pathway.

Whole-cell current clamp recordings were made using electrodes with DC resistances of 10-20MΩ. An intracellular pipette solution composed of (mM) 100 K-gluconate, 2

$MgCl_2$, 10 EGTA, 10 Hepes, 3 Na_2ATP, and 0.5 NaGTP with 0.1% Neurobiotin (Vector Laboratories Ltd, UK) was used. Only recordings with resting membrane potential (RMP) at a stable level between -45mV and -65mV were used for analyses. In all cases, only one intracellular recording was made in each animal. v.r. recordings were amplified through a Model 1700 A-M Systems differential AC amplifier (A-M Systems Inc., USA) filtered between 0.3kHz and 5kHz. Whole-cell recordings were made via an Axoclamp-2A patch clamp amplifier (Molecular Devices Inc., USA). All signals were sampled using a CED 1401 plus digitiser at 10 kHz and controlled using Signal (Cambridge Electronic Design Ltd., UK). Pharmacological substances were circulated in the saline or pressure-applied locally using a glass pipette with an opening of ~15μm positioned close to the recorded soma.

Analysis of v.r. and whole-cell recording traces was performed using DataView (© W.J. Heitler, University of St Andrews, UK) and data handled using Microsoft Excel (Microsoft Corporation, USA). Whole-cell recordings were analysed from raw files with the exception of firing threshold, which was analysed by determining derivatives to find the point of fastest rise time using DataView. Statistical analyses, in the form of Friedman's Two-Way Analysis of Variance or Wilcoxon Signed Rank Tests, were carried out using SPSS (IBM Corporation, USA) depending on the data distribution. Data are given as mean ± standard error.

In whole-cell recordings changes in the resting membrane potential (RMP), firing threshold and input resistance (R_{inp}) were measured in the presence of carbachol. The properties of the first action potential evoked by current injection was analysed with respect to spike peak depolarisation, half-height spike duration, AHP amplitude and

AHP duration. Using the DataView software, we first obtained the derivative of the whole-cell recording and then a secondary derivative was obtained from first derivative trace. The firing threshold was defined as the membrane potential at the time point when the second derivative peaked. Spike height was the membrane potential difference between spike peak and the threshold. AHP amplitude is the difference between the threshold and the maximum hyperpolarisation after spiking. In order to assess any potential change in transmitter release probability at RB synapses, the frequency of spontaneous synaptic potentials in dlis was analysed. This was done without applying TTX because tadpole spinal neurons seldom fire spontaneously. DC current was injected for a period of 5 minutes in each experimental condition to hold the membrane potential around or above IPSP reversal (~ -50 mV) to reveal EPSPs and IPSPs more clearly and to allow their amplitude measurements.

Recorded neurons were filled with 0.1% Neurobiotin by diffusion during intracellular recordings. Tadpoles were fixed overnight in 4% glutaraldehyde (Sigma-Aldrich, UK) after recordings. Tadpoles were first washed in phosphate buffer saline (PBS, pH 7.2) for five minutes, followed by two 15 minute washes in 1% Triton X100 (Sigma-Aldrich, UK) in PBS. Animals were then moved to a solution of 0.5% Triton X100 in PBS containing 0.3% ExtrAvidin Peroxidase (Sigma-Aldrich, UK) at room temperature for 3 hours. Tadpoles were again washed in PBS (four 10 minute washes) before being placed in a solution of 0.08% 3,3'-diaminobenzidine (DAB; Sigma-Aldrich, UK) in PB for 5 minutes in low light conditions. Animals were then moved to another solution of 0.08% DAB in PB containing 0.03% hydrogen peroxidase (Sigma-Aldrich, UK) for a further 5 minutes. The peroxidase oxidises the DAB producing a dark brown staining that can be visualised. To stop the DAB reaction the

animals were washed in tap water several times. Following DAB staining, dissections were carried out to further expose the nervous system. Remaining eyes, skin, muscle and yolk tissue was removed but the notochord was retained to provide structural support. Dehydration was carried out in a fume hood at room temperature. The dissected tadpoles were incubated three times in 100% alcohol for 3 minutes. They were then moved to a well of 99% Methyl benzoate (Sigma-Aldrich, UK) for 3 minutes and then incubated in 2 wells of 99% m-Xylene (Sigma-Aldrich, UK) for a further 3 minutes each. Tadpoles were then mounted on custom-made aluminium slides in DePex mounting medium (VWR International Ltd., UK). Slides were viewed on an upright microscope fitted with a drawing tube (Brunel Microscopes Ltd., UK). Some neurons were drawn by hand and others photographed using a Canon EX-FC100 camera. Composite photos were compiled using photos taken at different focal depths using Helicon Focus software. All figures were prepared using CorelDRAW X6 (Corel Corporation, USA).

Results

Swimming initiation threshold was increased by carbachol

We first examined the effect of bath-applied carbachol, a non-specific muscarinic receptor agonist, on swimming initiation thresholds. The majority of the trunk skin covering swimming muscles and spinal cord was removed to allow drug access to neurons in the central nervous system (Fig.1A). Fictive swimming was evoked by applying a 0.2ms current pulse to the head or tail skin. Threshold current was identified by increasing the current in small increments from 0. Following application

of 1µM carbachol, skin stimulation threshold was not changed. When the concentration of carbachol was increased to 3µM, skin stimulation threshold was increased (271.86 ± 113.07%; $p < 0.05$; $n = 5$) with a recovery to 109.31 ± 18.13% of control ($p > 0.05$; $n = 5$) in wash. At 10µM, 1 out of 6 tadpoles did not respond to skin stimulations up to a maximal 32mA whereas in the remaining 5 preparations, swimming could be evoked but there was frequent failed stimulation. In the successful trials where stimulation evoked swimming, the threshold increased to 433.55 ± 228.05% of control with little recovery in wash (484.49 ± 328.51%; $p < 0.05$; $n = 5$, Fig.1B). The activation of metabotropic receptors and second messenger signal pathways and its recovery is normally slow. However, it is unclear why there lacked any recovery within the washing off period in this case. At concentrations of 30µM ($n = 8$) and 100µM ($n = 5$), it was not possible to evoke fictive swimming by skin stimulation (up to 32 mA). Apart from the skin mechanosensory pathway, dimming light can activate the pineal eye pathway and start tadpole swimming (Roberts, 1978). In 5 of the 8 tadpoles where 30µM carbachol was applied, it was still possible to induce swimming by dimming the microscope illumination (Fig.1C). This suggests that the failure of skin stimuli to evoke swimming is at least partially due to inhibition of the mechanosensory pathway.

Effects of carbachol on RB neurons

We next made recordings from neurons in the mechanosensory pathway to identify the mechanisms of muscarinic inhibition of swimming thresholds. We chose to test the effects of 30 µM carbachol on neuronal properties since it had clear and consistent effects on swimming initiation. All sensory RB neurons have peripheral neurites

innervating tadpole trunk skin. Once these peripheral neurites are stimulated, action potentials propagate centrally to the RB neuron somata in the spinal cord and then along the central axons to excite sensory interneurons. Whole-cell patch-clamp recordings were made from 9 RB neurons at various locations along the length of the spinal cord, between the level of the 3rd and 10th myotomes. In all cases only one action potential was produced at the onset of current injection, which is the typical response of RB neurons (Fig.2A, (Winlove & Roberts, 2011)). Six of these preparations were exposed to 30µM carbachol, which was applied by bath circulation. In control RMPs of RB neurons were -52.8 ± 1.1 mV. RB input resistances (R_{inp}), derived from the current-voltage (I-V) relationship, were 1128 ± 293 MΩ below the rectification point (about the RMP level in most cases, R_{inp-}) and 289 ± 21 above the rectification point (R_{inp+}, Fig.2B). When 30µM carbachol was applied, RB resting properties (RMP and R_{inp}) and spike properties (threshold current, firing threshold, spike peak, half-height spike duration, AHP amplitude and duration) were not affected ($n = 6$, $p > 0.05$ in each case, Fig.2C,D). However, there is an increase in the R_{inp+} to 368 ± 27 MΩ in wash in comparison to control ($p < 0.05$, $n = 6$).

Effects of carbachol on dli properties

Having failed to detect muscarinic effects on RB neurons, we tested 30µM carbachol on the sensory interneurons in the mechanosensory pathway, which are located in the dorsolateral region of the spinal cord (dli). They included 5 dorsolateral commissural interneurons (dlcs) and 2 dorsolateral ascending interneurons (dlas) between the 3rd and 12th myotomes. dlis respond in similar ways to skin stimulation, are directly excited by RB neurons and receive IPSPs from aINs during swimming (Li *et al.*,

2002; 2004a). The effects of 30µM carbachol application were found to be similar in dlcs and dlas and therefore their data were pooled. dlis also typically show rectification in their I-V relationship, i.e. there is a deflection point near RMP (Li et al., 2004b). In control conditions, dli RMP was -54.2 ± 4.2 mV, while their R_{inp-} was 743 ± 130 MΩ and R_{inp+} was 360 ± 46 MΩ (R_{inp+}). All dlis responded to current injections by firing multiple action potentials (Fig.3A). A typical example of the I-V relationship of dlis can be seen in Fig.3B.

Carbachol at 30µM deepened dli RMP to -62.4 ± 3.6 mV ($p < 0.01$) with a recovery to -50.9 ± 3.4 mV but had no effect on R_{inp+} (348 ± 50 MΩ; $p > 0.05$). However, R_{inp-} was decreased to 521 ± 113 MΩ ($p < 0.05$; $n = 6$, Fig.3B, C). Similar to RBs, dli firing properties were not changed by 30µM ($p > 0.05$, $n = 6$ in each case, Fig.3D). These data indicate that mAChR activation in dlis may open some potassium channels and cause hyperpolarisation of dli RMP.

Effects of carbachol on the dli response to skin stimulation and spontaneous synaptic potentials

The effects of carbachol on dli resting properties should influence the role of dlis in relaying mechanosensory information from RBs to the swimming circuit and so contribute to the inhibition of swimming thresholds by carbachol. We therefore recorded dli responses to skin stimulation in the presence of carbachol. Five dlis were recorded from the same side of the body as the skin stimulation site. They fired reliable action potentials in response to skin stimulation. In the presence of 30µM carbachol, none of the 5 dlis displayed firing in response to skin stimulation. Only

subthreshold EPSPs were observed after skin stimulation (Fig.4A). The failure of dlis to fire spikes in carbachol may be a consequence of membrane potential hyperpolarisation and cellular input resistance decreases (Fig.3).

The suppression of dli spiking by carbachol may have alternatively resulted from a decreased vesicle release probability at RB synapses. We addressed this possibility by analysing the frequency and amplitude of spontaneous synaptic potentials in dlis. In each recording a 20s period was selected in which there was no ventral root activity. In control the EPSP frequency in 7 dlis was 1.16 ± 0.41Hz while the EPSP amplitude was 1.71 ± 0.65 mV. IPSP frequency in control was 0.85 ± 0.48Hz and the IPSP amplitude was 0.74 ± 0.34mV. In 30µM carbachol, no change was detected in these parameters ($p > 0.05$, $n = 7$ in each case, Fig.4B, C).

The effects of atropine on swimming initiation by skin stimulation and I-V rectification modulation

Endogenous activation of mAChRs in the mechanosensory pathway was investigated by bath-applying atropine, a general muscarinic antagonist. Skin stimulation led to fictive swimming in all concentrations of atropine tested. There was no change to the swimming initiation threshold by skin stimulation when atropine concentration was at 1, 3, 10 and 30 µM ($n = 5$, $p > 0.05$ in each case). Swimming threshold was reduced only by 100µM atropine to 51.12 ± 13.08% of the control current level ($p < 0.05$; $n = 6$, Fig.5A).

The general lack of effects of atropine on swimming threshold suggests that mAChRs on dlis are not endogenously activated at rest. The excitatory interneurons in the tadpoles swimming circuit, dINs, corelease glutamate and ACh to activate their corresponding ionotropic receptors (Li *et al.*, 2004b). dINs may be a potential source of cholinergic activation of muscarinic receptors on dlis although the synaptic connection probability is very low (Li *et al.*, 2007). We examined whether there was change in dli R_{inp} immediately after swimming and dINs released ACh to potentially activate mAChRs on dlis. Within 1.8 seconds after swimming ended, R_{inp-} decreased from 582 ± 108 MΩ in control to 547 ± 121 MΩ (n = 12 dlcs and 1 dla, $p < 0.05$, paired t-test) without affecting RMP, whereas R_{inp+} remained similar (from 480 ± 99 MΩ in control to 469 ± 99 MΩ, Fig.5B-E). As a result, I-V rectification ratio, measured by R_{inp-} divided by R_{inp+}, decreased from 1.27 ± 0.06 to 1.18 ± 0.06. However, this change in R_{inp-} was not affected by microperfused 20 μM atropine (n = 6, paired *t*-test, Fig.5F).

We recently showed that stimulating the head skin could activate some cholinergic interneurons in the brainstem which stopped swimming (Li *et al.*, 2017). We also tested R_{inp} within 3.5 seconds after repetitive head skin stimulation and its sensitivity to atropine. Following repetitive head skin stimulation (10 pulses at 30 Hz), there was no change in RMP (n =17, Fig.6A, B, paired *t*-test). R_{inp+} decreased from 436 ± 73 MΩ to 405 ± 69 MΩ ($p < 0.01$) and R_{inp-} decreased from 542 ± 73 MΩ to 428 ± 66 MΩ ($p < 0.001$, both n = 6, related sample Wilcoxon Signed Rank Test, Fig.6C). The opening of any ion channels could account for the decreases in R_{inp}. Interestingly, the conductance increase with negative step currents (0.82 ± 0.23 nS) test was larger than that for positive current tests (0.24 ± 0.09 nS, $p < 0.01$, related sample Wilcoxon

Signed Rank Test). This suggests the presence of multiple ionic mechanisms. The I-V rectification ratio also decreased from 1.24 ± 0.05 in control to 1.06 ± 0.04 following repetitive head skin stimulation (n = 17, p < 0.001, paired t-test). The decreased I-V rectification ratio was not affected by microperfused atropine at 20 µM (n = 6, related sample Wilcoxon Signed Rank Test, Fig.6D).

Discussion

The ubiquitous application of carbachol increased the swimming initiation threshold. Carbachol may target mAChRs in the sensory pathway or the swimming rhythm generation circuit. We recently found that activating M_2 receptors on dINs in the rostral hindbrain led to inhibition mediated by the G protein coupled inward-rectifying potassium channels and increase swimming thresholds (Li *et al.*, 2017). In this study, we have shown that activating mAChRs using carbachol can inhibit the mechanosensory interneurons and depress their responses to skin stimulation. Although carbachol is not highly selective to mAChRs over nAChRs, it has been widely used as a mAChR agonist. We did not see simultaneous decreases in R_{inp-} and R_{inp+} in RB neurons or dlis in the presence of carbachol, suggesting that both groups of neurons either lack nAChRs or that carbachol at 30 µM is selective to mAChRs. Previously, we showed that rhythmic neurons in the tadpole swimming circuit receive nAChR-mediated excitation from dINs (Li *et al.*, 2004b). When 10-50 µM carbachol was applied, there was no change in the R_{inp} of dINs (Li *et al.*, 2006). This provides indirect support that carbachol at up to 50 µM is selective to mAChRs in the tadpole swimming circuit.

What does carbachol modulate in the tadpole mechanosensory pathway? RBs and dlis both have rectification in their I-V responses (Li *et al.*, 2004a; Winlove & Roberts, 2012). It is unknown if this rectification arises from some outward-rectifying potassium currents (K_{or}, (Ketchum *et al.*, 1995)) or low voltage-activated potassium channels (Johnston *et al.*, 2010). Our data show carbachol reduces dli I-V rectification by specifically decreasing R_{inp-} and induces membrane potential hyperpolarisation. Previously in other preparations, the activation of M_2 and/or M_4 could open leak K^+ channels and hyperpolarise membrane potential (Egan & North, 1986), whereas M_1, M_3 and M_5 receptor activation can inhibit leak K^+ currents and consequently increase R_{inp} and depolarisation (Pitler & Alger, 1990; Uchimura & North, 1990; Wang & McKinnon, 1996; Broicher *et al.*, 2008). Our results suggest that mAChRs may also modulate K_{or} channels or low voltage-activated potassium channels, causing them to open at hyperpolarised potentials. Muscarinic modulation of non-cholinergic transmission has also been described previously (Quinlan & Buchanan, 2008; Bertrand & Cazalets, 2011; Mejia-Gervacio, 2012). Dlis receive glutamatergic excitation from RB neurons and rhythmic glycinergic inhibition from ascending interneurons (aINs) in the swimming circuit (Li *et al.*, 2002; 2004a). Our analyses of dli spontaneous synaptic potentials, however, showed no change in their frequency or amplitude in carbachol. This demonstrates a lack of presynaptic modulation of transmitter release from the sensory RB neurons and aINs. Neurons rhythmically active in tadpole swimming receive EPSPs from dlis but they also receive excitatory inputs from dINs. Similar analyses of spontaneous EPSPs in these neurons will thus not provide insights into potential presynaptic modulation of transmitter release at dli synapses.

The application of atropine shows the general lack of effects on swimming initiation thresholds in stage 37/38 tadpoles, suggesting the absence of endogenous mAChR activation in the mechanosensory pathway. Three types of cholinergic neurons have been pharmacologically identified in the stage 37/38 tadpole nervous system: motoneurons (Perrins & Roberts, 1995), dINs (Li *et al.*, 2004b) and the cholinergic cells in the brainstem responsible for the concussion-like behaviour (Li *et al.*, 2017). Among them, MNs have very ventral axons, not in a position to contact dli dendrites. Some dIN axons can be dorsal enough to contact more ventrally located dli dendrites. However, the probability of this type of synaptic connection is very low (Li *et al.*, 2007). The cholinergic neurons involved in concussion-like responses have been proposed to be located in the midbrain/rostral hindbrain region (Li *et al.*, 2017). We tested potential muscarinic action at the end of swimming and following repetitive head skin stimulation, which should activate the dINs and the cholinergic brainstem neurons, respectively. Interestingly, modulation of I-V rectification has been observed in both types of experiments but it is not sensitive to atropine application. The tadpoles we chose to study are still going through extensive developmental changes. Serotonergic receptors were previously shown to be expressed at stage 37/38 but their endogenous activation only appeared later in development (Sillar *et al.*, 1992). It is likely that the expression of muscarinic receptors precede the innervation of developing cholinergic fibres in the mechanosensory pathway in a similar way.

Author contributions

The experiments were designed W.-C. L. The data were collected and analysed by N.J.P. and W.-C. L. The paper was written by N.J.P. and W.-C. L.

Competing interests

The authors have no conflict of interest to declare.

Acknowledgement

This research was supported by a BBSRC studentship to N.J.P. and partially by a BBSRC grant to W.-C. L. (BB/L00111X)

References

Alaburda, A., Perrier, J.F. & Hounsgaard, J. (2002) An M-like outward current regulates the excitability of spinal motoneurones in the adult turtle. *J Physiol*, **540**, 875-881.

Arvidsson, U., Riedl, M., Elde, R. & Meister, B. (1997) Vesicular acetylcholine transporter (VAChT) protein: a novel and unique marker for cholinergic neurons in the central and peripheral nervous systems. *J Comp Neurol*, **378**, 454-467.

Bertrand, S.S. & Cazalets, J.R. (2011) Cholinergic partition cells and lamina x neurons induce a muscarinic-dependent short-term potentiation of commissural glutamatergic inputs in lumbar motoneurons. *Front Neural Circuits*, **5**, 15.

Broicher, T., Wettschureck, N., Munsch, T., Coulon, P., Meuth, S.G., Kanyshkova, T., Seidenbecher, T., Offermanns, S., Pape, H.C. & Budde, T. (2008) Muscarinic ACh receptor-mediated control of thalamic activity via G(q)/G (11)-family G-proteins. *Pflugers Arch*, **456**, 1049-1060.

Brownstone, R.M., Jordan, L.M., Kriellaars, D.J., Noga, B.R. & Shefchyk, S.J. (1992) On the regulation of repetitive firing in lumbar motoneurones during fictive locomotion in the cat. *Exp Brain Res*, **90**, 441-455.

Egan, T.M. & North, R.A. (1986) Acetylcholine hyperpolarizes central neurones by acting on an M2 muscarinic receptor. *Nature*, **319**, 405-407.

Fok, M. & Stein, R.B. (2002) Effects of cholinergic and noradrenergic agents on locomotion in the mudpuppy (Necturus maculatus). *Exp Brain Res*, **145**, 498-504.

Guertin, P.A. & Hounsgaard, J. (1999) L-type calcium channels but not N-methyl-D-aspartate receptor channels mediate rhythmic activity induced by cholinergic agonist in motoneurons from turtle spinal cord slices. *Neurosci Lett*, **261**, 81-84.

Huang, A., Noga, B.R., Carr, P.A., Fedirchuk, B. & Jordan, L.M. (2000) Spinal cholinergic neurons activated during locomotion: localization and electrophysiological characterization. *J Neurophysiol*, **83**, 3537-3547.

Johnston, J., Forsythe, I.D. & Kopp-Scheinpflug, C. (2010) Going native: voltage-gated potassium channels controlling neuronal excitability. *J Physiol*, **588**, 3187-3200.

Ketchum, K.A., Joiner, W.J., Sellers, A.J., Kaczmarek, L.K. & Goldstein, S.A. (1995) A new family of outwardly rectifying potassium channel proteins with two pore domains in tandem. *Nature*, **376**, 690-695.

Li, W.C., Cooke, T., Sautois, B., Soffe, S.R., Borisyuk, R. & Roberts, A. (2007) Axon and dendrite geography predict the specificity of synaptic connections in a functioning spinal cord network. *Neural Dev*, **2**, 17.

Li, W.C., Soffe, S.R. & Roberts, A. (2002) Spinal inhibitory neurons that modulate cutaneous sensory pathways during locomotion in a simple vertebrate. *J Neurosci*, **22**, 10924-10934.

Li, W.C., Soffe, S.R. & Roberts, A. (2004a) Dorsal spinal interneurons forming a primitive, cutaneous sensory pathway. *J Neurophysiol*, **92**, 895-904.

Li, W.C., Soffe, S.R. & Roberts, A. (2004b) Glutamate and acetylcholine corelease at developing synapses. *Proc Natl Acad Sci U S A*, **101**, 15488-15493.

Li, W.C., Soffe, S.R., Wolf, E. & Roberts, A. (2006) Persistent responses to brief stimuli: feedback excitation among brainstem neurons. *J Neurosci*, **26**, 4026-4035.

Li, W.C., Zhu, X.Y. & Ritson, E. (2017) Mechanosensory Stimulation Evokes Acute Concussion-Like Behavior by Activating GIRKs Coupled to Muscarinic Receptors in a Simple Vertebrate. *eNeuro*, **4**.

Mejia-Gervacio, S. (2012) Muscarinic control of AMPA receptor responsiveness in mouse spinal cord motoneurons. *J Physiol*, **590**, 4663-4671.

Mentis, G.Z., Alvarez, F.J., Bonnot, A., Richards, D.S., Gonzalez-Forero, D., Zerda, R. & O'Donovan, M.J. (2005) Noncholinergic excitatory actions of motoneurons in the neonatal mammalian spinal cord. *Proc Natl Acad Sci U S A*, **102**, 7344-7349.

Miles, G.B., Hartley, R., Todd, A.J. & Brownstone, R.M. (2007) Spinal cholinergic interneurons regulate the excitability of motoneurons during locomotion. *Proc Natl Acad Sci U S A* **104:**, 2448-2453.

Nieuwkoop, P.D. & Faber, J. (1956) *Normal tables of Xenopus laevis (Daudin)*, Amsterdam: North Holland.

Nishimaru, H., Restrepo, C.E., Ryge, J., Yanagawa, Y. & Kiehn, O. (2005) Mammalian motor neurons corelease glutamate and acetylcholine at central synapses. *Proc Natl Acad Sci U S A*, **102**, 5245-5249.

Panchin Yu, Y., Perrins, R.J. & Roberts, A. (1991) The action of acetylcholine on the locomotor central pattern generator for swimming in Xenopus embryos. *J Exp Biol*, **161**, 527-531.

Perrins, R. & Roberts, A. (1994) Nicotinic and muscarinic ACh receptors in rhythmically active spinal neurones in the Xenopus laevis embryo. *J Physiol*, **478 (Pt 2)**, 221-228.

Perrins, R. & Roberts, A. (1995) Cholinergic and electrical synapses between synergistic spinal motoneurones in the Xenopus laevis embryo. *J Physiol* **485**, 135-144.

Pitler, T.A. & Alger, B.E. (1990) Activation of the pharmacologically defined M3 muscarinic receptor depolarizes hippocampal pyramidal cells. *Brain Res*, **534**, 257-262.

Quinlan, K.A. & Buchanan, J.T. (2008) Cellular and synaptic actions of acetylcholine in the lamprey spinal cord. *J Neurophysiol*, **100**, 1020-1031.

Quinlan, K.A., Placas, P.G. & Buchanan, J.T. (2004) Cholinergic Modulation of the Locomotor Network in the Lamprey Spinal Cord. *J Neurophysiol*, **92**, 1536-1548.

Roberts, A. (1978) Pineal eye and behaviour in Xenopus tadpoles. *Nature*, **273**, 774-775.

Schmidt, B.J. (1994) Afterhyperpolarization modulation in lumbar motoneurons during locomotor-like rhythmic activity in the neonatal rat spinal cord in vitro. *Exp Brain Res*, **99**, 214-222.

Sherriff, F.E. & Henderson, Z. (1994) A cholinergic propriospinal innervation of the rat spinal cord. *Brain Res*, **634**, 150-154.

Sillar, K.T., Wedderburn, J.F. & Simmers, A.J. (1992) Modulation of swimming rhythmicity by 5-hydroxytryptamine during post-embryonic development in Xenopus laevis. *Proc R Soc Lond B Biol Sci*, **250**, 107-114.

Smetana, R., Juvin, L., Dubuc, R. & Alford, S. (2010) A parallel cholinergic brainstem pathway for enhancing locomotor drive. *Nat Neurosci*, **13**, 731-738.

Smetana, R.W., Alford, S. & Dubuc, R. (2007) Muscarinic receptor activation elicits sustained, recurring depolarizations in reticulospinal neurons. *J Neurophysiol*, **97**, 3181-3192.

Uchimura, N. & North, R.A. (1990) Muscarine reduces inwardly rectifying potassium conductance in rat nucleus accumbens neurones. *J Physiol*, **422**, 369-380.

Wang, H.S. & McKinnon, D. (1996) Modulation of inwardly rectifying currents in rat sympathetic neurones by muscarinic receptors. *J Physiol*, **492 (Pt 2)**, 467-478.

Wilson, J.M., Rempel, J. & Brownstone, R.M. (2004) Postnatal development of cholinergic synapses on mouse spinal motoneurons. *J Comp Neurol*, **474**, 13-23.

Winlove, C.I. & Roberts, A. (2011) Pharmacology of currents underlying the different firing patterns of spinal sensory neurons and interneurons identified in vivo using multivariate analysis. *J Neurophysiol*, **105**, 2487-2500.

Winlove, C.I. & Roberts, A. (2012) The firing patterns of spinal neurons: in situ patch-clamp recordings reveal a key role for potassium currents. *Eur J Neurosci*, **36**, 2926-2940.

Yung, K.K. & Lo, Y.L. (1997) Immunocytochemical localization of muscarinic m2 receptor in the rat spinal cord. *Neuroscience Letters*, **229**, 81-84.

Zagoraiou, L., Akay, T., Martin, J.F., Brownstone, R.M., Jessell, T.M. & Miles, G.B. (2009) A cluster of cholinergic premotor interneurons modulates mouse locomotor activity. *Neuron*, **64**, 645-662.

Figure 1 Experimental setup and the effects of carbachol on swimming thresholds. **A**. Experimental setup showing the arrangement of electrodes and the microperfusion pipette. Dotted line outlines the regions of tissue dissected away to expose swimming myotomes (m) and the spinal cord (sc). **B**. Stimulation threshold (as % of control) in the presence of 1µM, 3µM and 10µM carbachol. * denotes significance at $p<0.05$. **C**. Skin stimulation (arrow heads, control at 2µA, carbachol at 32mA, wash with partial recovery at 10µA) fails to start swimming in the presence of 30µM Carbachol. Light dimming (horizontal bars) evokes two brief fictive swimming bouts.

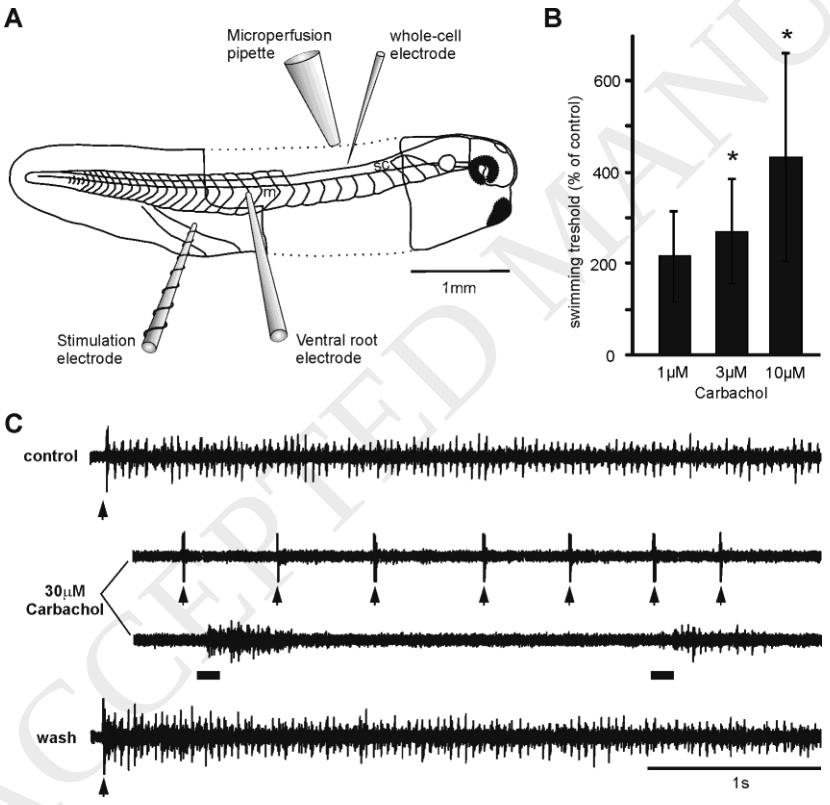

Figure 2. The effects of 30µM carbachol on RB neuron properties. **A**. Typical RB responses to step current injections. **B.** I-V relationship of a typical RB neuron in control, carbachol and wash. Note the deflection point in the plot around the RMP. **C**. RB neuron RMP and R_{inp} are not affected by carbachol but there is some unexplained increase in R_{inp+} in wash (*). **D**. RB spike properties are unaffected by Carbachol. Black bars are control, unfilled ones are carbachol and grey ones wash in **C** and **D**. * denotes $p < 0.05$.

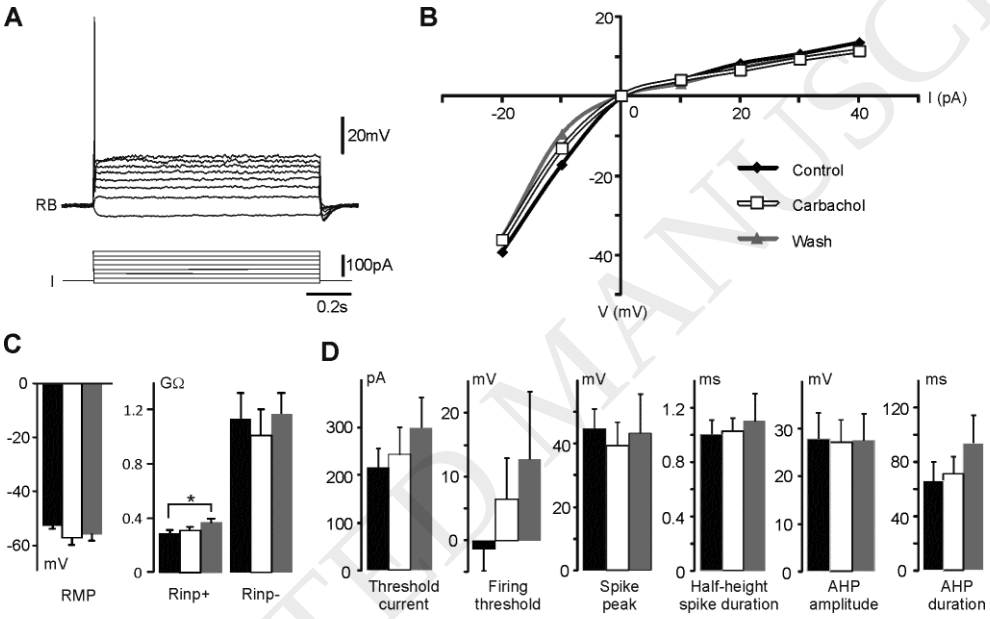

Figure 3. The effects of 30µM Carbachol on dli properties. **A**. A dlc's responses to step current injections. **B**. I-V relationship of a dlc in control, carbachol and wash. **C**. Summary of dli RMP and R_{inp} calculated above and below the deflection point. **D**. dli spike properties are unaffected by Carbachol. Black bars: control; unfilled bars: carbachol; grey bars: wash (**C** and **D)**. * denotes $p < 0.05$ and ** $p < 0.01$.

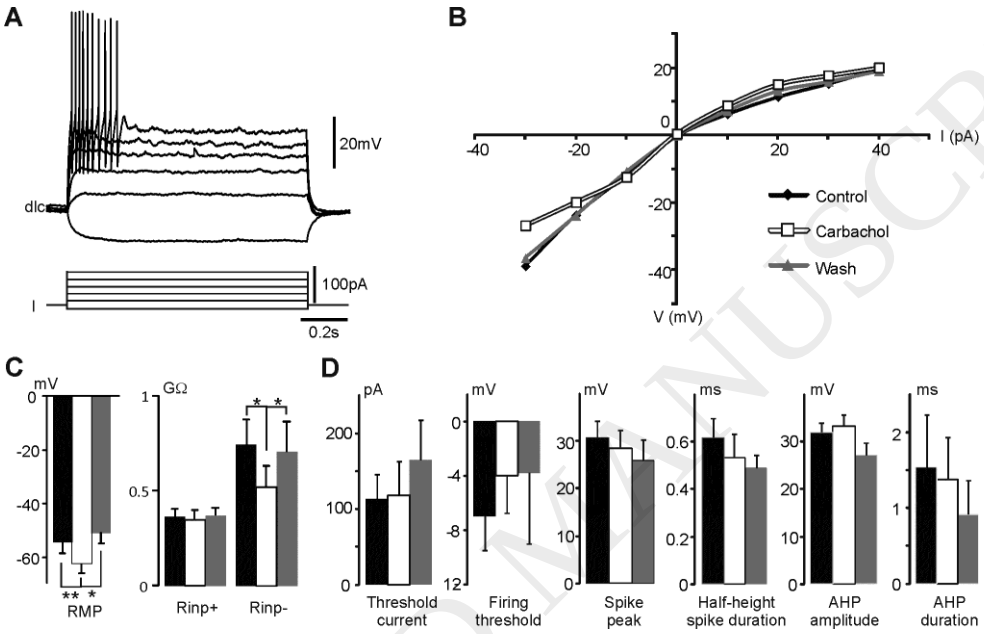

Figure 4. The effects of 30μM carbachol on dli spiking after skin stimulation and spontaneous synaptic potentials. **A**. Responses of a dli to skin stimulation (arrow) in control, carbachol and wash. * indicates the failure of spiking. **B**. Carbachol does not influence spontaneous EPSP Frequency or Amplitude in dlis. **C**. Spontaneous IPSP frequency or Amplitude is not changed by carbachol.

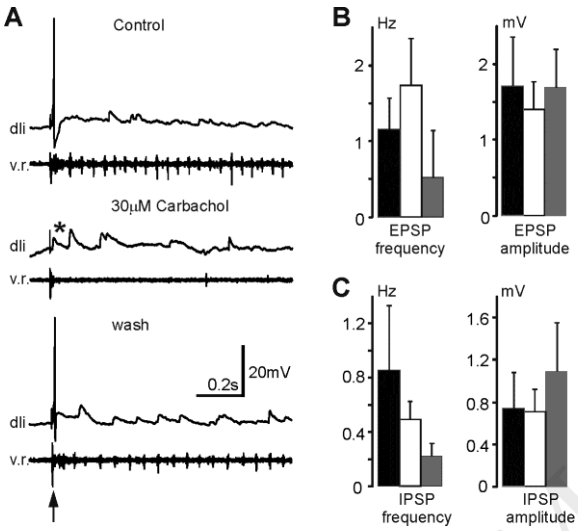

Figure 5. Effects of atropine on the swimming threshold and dli R_{inp} immediately after swimming. **A**. Effect of atropine on swimming initiation thresholds (as % of control) in 1 - 100µM atropine. Numerals inside bars are numbers of animals used for each concentration. **B**. R_{inp} of a dlc before and after swimming (v.r., with middle period removed), tested using ± 30 pA current steps (*). **C**. Neurobiotin staining of the dlc recorded in B. Dotted lines indicates the dorsal and ventral edges of the spinal cord. Arrow head points at the ascending branch of the dlc commissural axon. **D**. There is no change in RMP after swimming. **E**. R_{inp-} but not R_{inp-}decreases after swimming. **F**. Atropine at 20µM does not block the post-swimming R_{inp-} decrease. * indicates $p < 0.05$ in A and E.

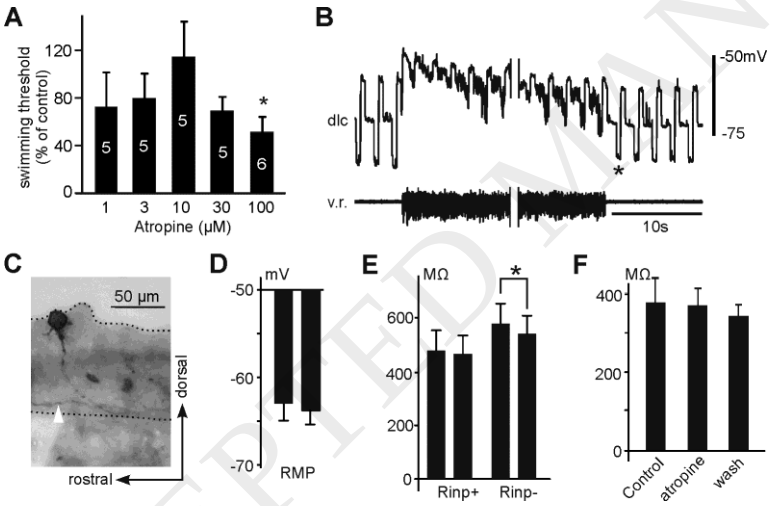

Figure 6. Modulation of the dli R_{inp} following repetitive head skin stimulation. **A**. Testing R_{inp} of a dlc using ± 80 pA current steps (*) before and after repetitive head skin stimulation (double arrows, 10 pulses at 30 Hz). Action potentials are truncated. **B**. There is no change in dli RMPs after swimming. **C**. Both R_{inp+} and R_{inp-}decrease after head skin stimulation. ** indicate significance at $p < 0.01$. **D**. Atropine does not alter I-V rectification ratio after head skin stimulation.